DOE/NASA/0176-81/4
CR 165519

PREPARATION AND EVALUATION OF ADVANCED ELECTROCATALYSTS FOR PHOSPHORIC ACID FUEL CELLS

7TH QUARTERLY REPORT

Paul Stonehart, John Baris, John Hochmuth and Peter Pagliaro

July - September 1981

PREPARED FOR:

NATIONAL AERONAUTICS AND SPACE ADMINISTRATION
Lewis Research Center
Under Contract DEN-3-176
Prepared Under Interagency Agreement DEAI-03-80ET17088

FOR:

U.S. DEPARTMENT OF ENERGY
Energy Technology
Division of Fossil Fuel Utilization

stonehart associates

17 Cottage Road, Madison, Connecticut 06443
Telephone Area Code 203 245-7507

1. Report No.	2. Government Accession No.	3. Recipient's Catalog No.
NASA CR 165519		

4. Title and Subtitle	5. Report Date
PREPARATION AND EVALUATION OF ADVANCED ELECTRO-CATALYSTS FOR PHOSPHORIC ACID FUEL CELLS	September 30, 1981
	6. Performing Organization Code

7. Author(s)	8. Performing Organization Report No.
Dr. Paul Stonehart John Baris, John Hochmuth and Peter Pagliaro	
	10. Work Unit No.

9. Performing Organization Name and Address	11. Contract or Grant No.
STONEHART ASSOCIATES, INC. 17 Cottage Road - P.O. Box 1220 Madison, CT 06443	DEN-3-176
	13. Type of Report and Period Covered
	Contractor Report

12. Sponsoring Agency Name and Address	14. Sponsoring Agency Code
U.S. Department of Energy Energy Technology Division of Fossil Fuel Utilization	DOE/NASA/0176-81/4

15. Supplementary Notes

7th Quarterly Report Mail Stop 49-5, NASA-Lewis Research Center
Project Manager: Dr. M. Lauver, 21000 Brookpark Road, Cleveland, Ohio 44135
Prepared Under Interagency Agreement DEAI-03-80ET17088

16. Abstract

A number of new electrocatalyst combinations were prepared and characterized. These electrocatalysts were formulated to contain platinum combined with transition metal carbide forming elements (W, Mo, V) for cathodes and platinum combined with palladium for anodes. The metals were supported on Consel I and Consel IV which were developed in our parallel EPRI 1200-2 program. High resolution electron microscopy was used to determine the crystallite size and dispersion of platinum-palladium alloy electrocatalysts in order to provide analytical support for the electrochemical determinations of the particle dispersions. An equation has been derived which correlates palladium crystallite size with electrochemical hydrogen adsorption. Based on comparisons of electrocatalyst performances in the presence of pure hydrogen and hydrogen containing carbon monoxide, it was shown that the apparent poisoning of the electrocatalyst by carbon monoxide is influenced by the electrode structure. This conclusion is extremely important since further gains in electrode performance will be obtained by improvements in the electrocatalyst-PTFE structure to reduce the thickness of the electrolyte films on the electrocatalysts in fuel cell electrodes. This work is not yet capable of predicting the gains that may be possible by more effectively utilizing the electrocatalyst.

17. Key Words (Suggested by Author(s))	18. Distribution Statement
fuel cells; electrocatalysts; electrochemical power generation; phosphoric acid	Unclassified - unlimited STAR Category 44

19. Security Classif. (of this report)	20. Security Classif. (of this page)	21. No. of Pages	22. Price*
Unclassified	Unclassified	27	

* For sale by the National Technical Information Service, Springfield, Virginia 22161

TABLE OF CONTENTS

ABSTRACT

A number of new electrocatalyst combinations were prepared and characterized. These electrocatalysts were formulated to contain platinum combined with transition metal carbide forming elements (W, Mo, V) for cathodes and platinum combined with palladium for anodes. The metals were supported on Consel I and Consel IV which were developed in our parallel EPRI 1200-2 program. High resolution electron microscopy was used to determine the crystallite size and dispersion of platinum-palladium alloy electrocatalysts in order to provide analytical support for the electrochemical determinations of the particle dispersions. An equation has been derived which correlates palladium crystallite size with electrochemical hydrogen adsorption. Based on comparisons of electrocatalyst performances in the presence of pure hydrogen and hydrogen containing carbon monoxide, it was shown that the apparent poisoning of the electrocatalyst by carbon monoxide is influenced by the electrode structure. This conclusion is extremely important since further gains in electrode performance will be obtained by improvements in the electrocatalyst-PTFE structure to reduce the thickness of the electrolyte films on the electrocatalysts in fuel cell electrodes. This work is not yet capable of predicting the gains that may be possible by more effectively utilizing the electrocatalyst.

1. Objective and Scope of Work

The overall objective of this electrocatalysis program is to define the feasibility of lowering the electrocatalyst cost and to increase the activity in phosphoric acid fuel cells, as a way to increase the commercial viability of fuel cells for producing electric power.

The specific objectives of the present tasks are the preparation of a series of high surface area electrocatalysts for evaluation in phosphoric acid fuel cells. This involves fabrication of efficient gas-diffusion electrode structures and determining their electrochemical parameters for hydrogen oxidation and oxygen reduction. When possible, new experimental techniques and theoretical interpretations will be forwarded towards an understanding of the relevant electrochemical parameters.

2. Summary of Previous Work

Previously, two areas of electrocatalyst formulations have been developed. The first area concerns anode electrocatalysts for operation in hot phosphoric acid in the presence of electrocatalyst poisons contained in the anode gas feed stream. The principal poisons are carbon monoxide and hydrogen sulphide. Binary alloy combinations of platinum with another element have been prepared on partially graphitized carbon supports. Patent applications have now been filed by DOE. These catalyst formulations perform as well as pure platinum supported on carbon but with a decrease in the electrocatalyst cost of 50-80%.

These cost savings that have been achieved so far are significant, since at the present time, 1 MW of power generated by fuel cells can require between 3 to 5 kg of platinum. (This calculation is based on 0.75 mg of platinum/cm^2 of cell operating at 200 mA at a terminal voltage of 0.65 V or 300 mA at a terminal voltage of 0.75 V.) A conservative projection for U.S. installed capacity is 15,000 MW cumulative through the year 2000 and an equal amount worldwide. This would require between 90,000 and 150,000 kg of platinum. Based on present prices of $450 per troy ounce and 32 troy ounces per kg, this represents a platinum requirement of $1,296,000,000 to $2,160,000,000 (1981 base). The potential savings in catalyst cost to the year 2000 are then between $259,200,000 and $432,000,000 (1981 base). The price of platinum may well increase above $450 per troy ounce, but this may be offset by a smaller market development. The cost savings are then expected to be constant.

For the oxygen electrode, platinum combined with a transition metal carbide forming element (W, Mo, V) has been constructed on partially graphitized carbon supports (Consel IV). The Consel IV was developed in a parallel EPRI 1200-2 program. These electrocatalyst formulations show 755 mV versus hydrogen at 100 ASF on air at 180°C and indicate a potential improvement to 775 mV versus hydrogen with improved electrode structures. Under pressurized fuel cell conditions (UTC at 5 atm) this would give 805 mV at 320 ASF for 180°C (iR free). With an electrocatalyst performance diagnostic under oxygen at 900 mV versus hydrogen, the current density is 44 mA/mg of platinum, which is projected to reach 60 mA/mg of platinum with improved electrode structures. Patent disclosures have been documented in this area on behalf of DOE.

The catalyst preparations for this quarterly report are summarized in the following table.

TABLE I

Catalyst #	Metals	Alloy Mix w/o	Total Load w/o	Support	Heat Treatment
EC-149	PtS	10.0	10	Consel I	200°C H_2/N_2
EC-150	Pd/Nb	10.0/2.91	12.9	Consel I	900°C H_2/N_2
EC-151	Pd/Ta	10.0/4.25	14.3	Consel I	900°C H_2/N_2
EC-152	Pt/Ta	10.0/2.32	12.3	Consel I	900°C H_2/N_2
EC-216	Pt	10.0	10.0	Consel IV	200°C H_2/N_2
EC-217	Pt	10.0	10.0	Consel IV	900°C H_2/N_2
EC-214	Pt/V	9.9/0.9	10.8	Consel I	900°C H_2/N_2
EC-215	Pt/V	9.9/0.9	10.8	Vulcan XC-72R	900°C H_2/N_2
EC-154	Pt/V	9.9/0.9	10.8	Consel IV	
EC-155	Pt	--	5	Consel I	
EC-156	Pt	--	5	Consel IV	
EC-157	Pt/V	4.96/0.43	5.4	Consel IV	

3.6. Task 6 - Characterization of Platinum-Based Carbon-Supported Electrocatalysts

Voltammetry is being used to get an initial impression of the characteristics of the above catalysts. Although pre- and post-performance test voltammetry on these catalysts is not yet complete, some preliminary data can be reported.

As an estimate of the platinum or palladium surface area, the hydrogen adsorption pseudocapacity analysis has been used (Stonehart, Power Sources, 514, 1966). The following table summarizes the voltammetry obtained to date.

TABLE II

Catalyst #	Composition/Support	Surface Area (m^2/g) Pre-Test	Post-Test	% SA Lost
EC-149	10% PtS/Consel I	82		
EC-150	12.9% Pd-Nb/Consel I	88	54	38
EC-151	14.3% Pd-Ta/Consel I	128	95	26
EC-152	12.3% Pt-Ta/Consel I	20	10	50
EC-216	10% Pt/Consel IV	125	80	36
EC-217	10% Pt/Consel IV	60	60	0
EC-214	10.8% Pt_3V/Consel I	75		
EC-215	10.8% Pt_3V/Vulcan	100		

Since none of the voltammetric curves are substantially different from curves of platinum or palladium, they will not be included in this report. Voltammetry can only give an estimate of the surface area of alloy catalysts and tells nothing of the surface composition when the alloying element does not produce a measurable feature on the voltammetric curve. Further characterization of these alloy catalysts must proceed with microscopy or surface spectroscopy. Even these techniques are often stretched to their limits when applied to highly dispersed supported catalysts.

Earlier this year, work on this contract produced several hydrogen oxidation binary alloy electrocatalysts which performed exemplarily, especially in the presence of carbon monoxide. The platinum-palladium electrocatalysts showed superior performance over pure platinum catalysts and were able to perform with minimal loss due to carbon monoxide poisoning even with carbon monoxide levels as high as 30%. At the request of NASA and DOE, patent disclosures have been written and a patent application (DOE Case S-55,310) has now been submitted.

At that time, the only technique available for characterizing the surface areas of these catalysts was electrochemical. Voltammetry was used extensively in an attempt to obtain crystallite size information. Since palladium will absorb hydrogen as well as adsorb it, then surface area determinations by this method are ambiguous. The voltammetric data needed to be verified by additional techniques. The gas phase carbon monoxide adsorption technique provided no aid, since it produced data which was both incomprehensible and non-reproducible. An explanation for this has not yet been found.

High resolution electron microscopy was used as a preferred technique. The platinum-palladium system was of sufficient interest to warrant the investment of time and resources to produce the required high magnification photomicrographs. Figures 1 and 2 are examples of this work. The magnification on these photomicrographs is 2 X 10^6 times (2,000,000X). Each millimeter is equivalent to 5 Å.

Figures 1 and 2 are quarter tone reproductions of photographic prints, so some of the fine resolution in the original photographic print is lost. The transmission electron micrograph plates were obtained at a magnification of 400,000X and then 5X enlargements were produced from selected areas of the plates to the prints. It can be seen by comparison of Figures 1 and 2 that the metal crystallite sizes of the Pd particles in Figure 1 are larger than the Pt-Pd alloy particles of Figure 2. Table II shows that our catalyst preparation techniques produce a higher dispersion for platinum than palladium. These electron micrographs demonstrate that the addition of platinum to the palladium (Figure 2, EC 123, is a 50/50 a/o Pt/Pd alloy) confers a significantly higher dispersion to the palladium than for palladium alone. Based on the transparency of the metal particles to the electron beam, some idea can be gained for the metal particle thickness. Figure 1 (EC 125) shows uniform densities for the particles, arguing that the apparently spherical particles are of approximately equal size and thickness. The metal particles in Figure 2 (EC 123) on the other hand, show significant variation in size and electron transparency, suggesting thin platelets.

One further feature of the electrocatalysts is exhibited by these electron micrographs. Close examination of the carbon support surface shows distinct evidence for graphitic layers. (Parallel lines 3.5 Å width separation). This demonstrates that the Consel I support that is so beneficial, has the surface graphitic character that is required for both corrosion resistance in the hot phosphoric acid and for stabilizing the PGM crystallites. The interior of the carbon particle remains untouched in a more turbostratic form to preserve the integrity of the carbon agglomerate.

Table III summarizes the data obtained from these photomicrographs. Each of the catalysts listed in Table II was examined extensively at both low and high magnification in order to produce 5 to 6 high magnification photomicrographs of each for analysis.

FIGURE 1. EC 125 4 w/o Pd on Consel I. 2,035,000X mag.

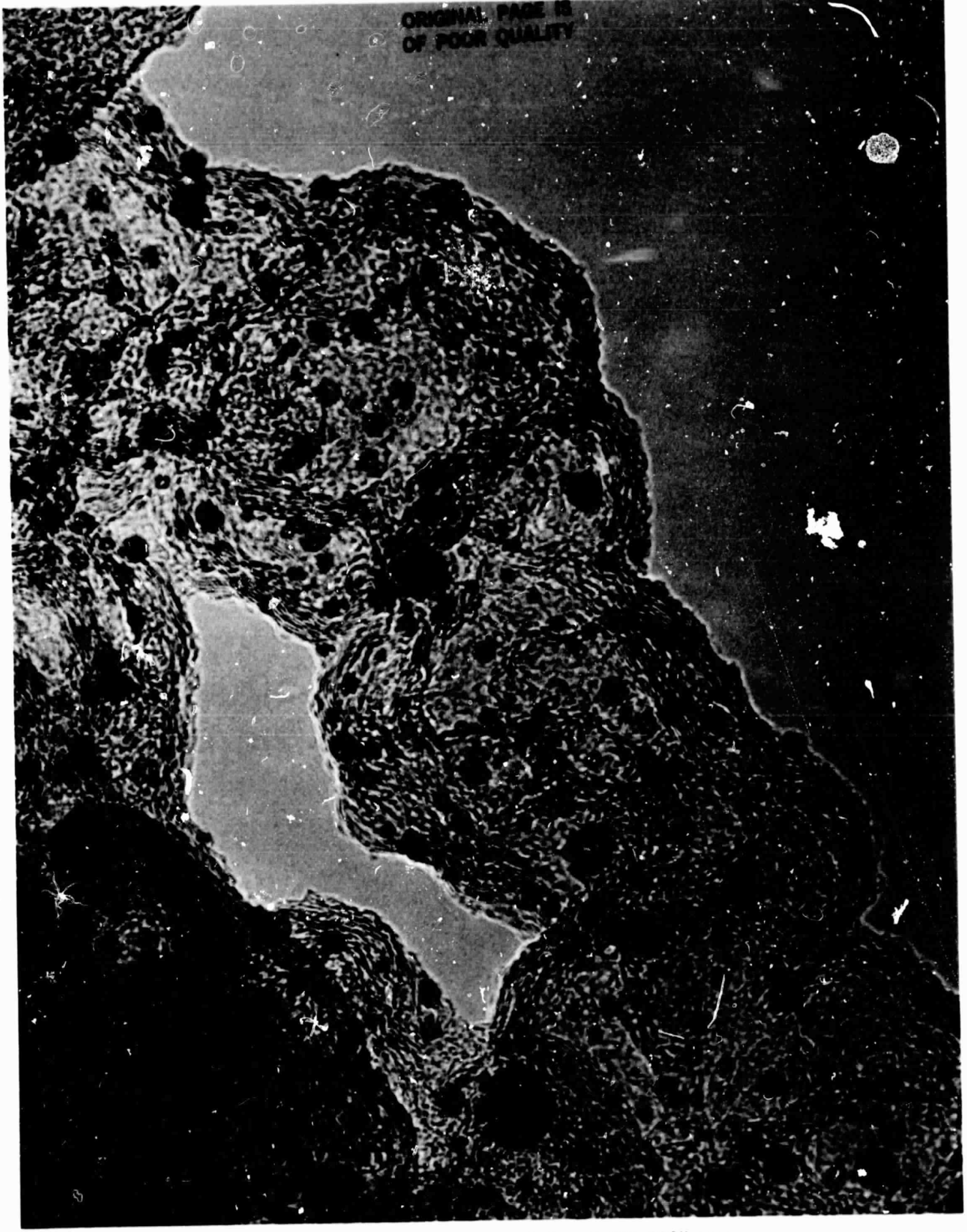

FIGURE 2. EC 123 4 w/o Pt-Pd (50 a/o Pd) on Consel I. 2,035,000X mag.

TABLE III

Catalyst #	Catalyst	Crystallite Size (Å) ECA	Crystallite Size (Å) Microscopy
EC 127	4% Pt/Consel I	15 Å	17 ± 3 Å
EC 125	4% Pd/Consel I	19 Å	40 ± 10 Å
	4% PGM/Consel I		
EC 122	a. 25 a/o Pt/Pd	33 Å	50 ± 25 Å
EC 123	b. 50 a/o Pt/Pd	21 Å	25 ± 3 Å
EC 128	c. 75 a/o Pt/Pd	18 Å	30 ± 15 Å

An estimate of this size distribution is included in Table III. The crystallite size determinations by voltammetry and microscopy are in very good agreement for 4% Pt/Consel I as would be expected. The voltammetry underestimates the crystallite size when palladium is present. This is due to the absorption of hydrogen by internal palladium to form palladium hydride. In fact, the hydrogen to palladium absorption ratio can now be determined. Equation (1) below (see Appendix for derivation) relates the charge measured under the hydrogen region for the palladium voltammogram with the crystallite size, assuming spherical geometry.

$$d = \frac{B(1-R)}{Q-AR} \qquad (1)$$

where Q is the charge (per gram of palladium) measured under the cathodic hydrogen peak on a voltammogram; A and B are constants, ($A = 9.07 \times 10^2$, $B = 1.10 \times 10^4$); R is the atomic ratio of hydrogen to palladium atoms interior to the crystallite; and d is the diameter of the crystallite in angstroms. The surface H/Pd ratio is assumed to be 1. Using 40 Å as d and 546 coul/gram Pd measured previously, the ratio R is equal to 0.43.

During voltammetry, then, the H/Pd ratio interior to a crystallite is equal to 0.43 (subject to further experimental verification) which is somewhat lower than 0.6 reported by Palcyewska (Advances in Catalysis, 24, 247-253) for bulk palladium in the gas phase. This is, perhaps, an example of the strangeness in the properties of small particles versus the properties of the bulk material, where the surface energy of the particle is affecting the bulk properties of the material.

The value of R needs to be verified by further correlations of voltammetry and microscopy on other crystallite sizes of palladium, but once that is done, Equation (1) can be used to determine palladium crystallite size by voltammetry.

Of the three platinum-palladium catalysts reported in TableIII, the 50 a/o Pt/Pd catlayst has the smallest average crystallite diameter with the most uniform dispersion (Figure 2). This may, in part, explain the fact that a 50 a/o Pt/Pd ratio also gives the best performance with the highest CO poisoning tolerance (see January report, Figure 10).

A 50 a/o Pt/Pd ratio would also be expected to give the most homogeneous alloy composition. Perhaps the non-uniformity of the 25 a/o and 75 a/o Pt/Pd catalysts is due to an excess of Pt or Pd producing unalloyed Pt or Pd crystallites when Pt or Pd is in excess over a 50 a/o mix. Such an inhomogeneous catalyst would not be expected to take full advantage of the synergism which seems to exist between platinum and palladium for CO tolerance.

3.7. Task 7 - Catalytic Activity of Platinum-Based Carbon-Supported Electrolytes Cathodes

Consel IV, an advanced support material, developed under the Stonehart Associates EPRI-1200-2 program, shows excellent promise as a catalyst support for platinum-vanadium intermetallic catalysts as shown in Quarterly Report #6 of this contract. It also shows promise as a support for platinum electrocatalysts. Although some improvement could be made in the preparation technique to produce a higher surface area catalyst, the performance of this catalyst as a cathode is promising, as shown in Figure 3.

Preparation of platinum-vanadium on Vulcan XC-72R (EC-215) produced an excellent electrocatalyst. The cathodic performance curve, shown in Figure 4, is as good as the best platinum on Vulcan electrocatalyst.

The performance of catalyst EC-149 (PtS/Consel I) is much improved over previous platinum sulphide catalysts. The Tafel slope for oxygen reduction at 180°C in 100% H_3PO_4 is 115 mV/decade; the activity is 14 mA/mg PtS, and the potential at 200 mA/cm^2 on air is 651 mV (vs H_2). Although this does not yet match the performance of platinum alone, it is much improved over previous preparations of platinum sulphide (See 6th Quarterly Report).

The addition of tantalum and niobium to palladium did not improve its catalytic activity as either a cathode or an anode. Palladium on Consel I will operate as an anode at 200 mA/cm^2 and give a potential of 11 mV (vs H_2) and will operate at 250 mV (vs H_2) at 200 mA/ cm^2 on air.

The addition of niobium decreased the anode performance to 156 mV at 200 mA/cm^2 and the cathode performance was so poor that it would not operate at 200 mA/cm^2 on air. The addition of tantalum produced similarly poor results. The hope that the addition of tantalum or niobium would produce a more platinum-like performance is obviously not yet realized. It must be remembered that this was an initial attempt to produce palladium intermetallic and improved preparations may be possible.

Catalyst EC-152, a platinum-tantalum intermetallic on Consel I, has performance characteristics which are not as good as platinum on Consel I by itself. At 200 mA/cm^2 a 0.5 mg/cm^2 loaded electrode of EC-152 operates at a potential of 590 mV in 180°C, 100% H_3PO_4 (vs > 700 mV for platinum on Consel I).

Anodes

Due to interest in the use of methanol as a fuel cell fuel for transportation (Los Alamos) and for man-pack Army power systems (Fort Belvoir), it is of some considerable importance that the performances of advanced electrocatalysts and electrode structures be evaluated. Methanol has the distinct advantage that it is water soluble and, therefore, the water for the steam reforming may be added to the fuel prior to introduction to the steam reformer itself. This leads to system simplicity. The effluent from a steam reformer with methanol and water as the fuel is 75% H_2, 0.5% CO, and 24.5% CO_2, showing a lower carbon monoxide concentration than steam reformed hydrocarbons.

We have performed polarization tests using a methanol steam reformate gas mixture with the platinum-palladium alloy (50 a/o Pt) supported on Consel I that was previously developed. In order to flex the performance curves and to use the carbon monoxide concentration as a probe for the electrode structure and electrocatalyst performance (which will be described more fully later), the electrode performance characteristics on hydrogen containing up to 5% carbon monoxide were obtained. This provided a bracketing for the carbon monoxide poisoning curves that were obtained previously for hydrogen oxidation on platinum electrocatalysts where the carbon monoxide poisoning levels ranged from 1% to 30%. Anode performance curves as a function of carbon monoxide partial pressure and temperature with 75% H_2 are shown in Figures 5 through 8.

In Figures 5 through 8 it should be noted that for 75% H_2 the open circuit potential at 180°C must be 7 mV from the reversible H_2 potential when p_{H_2} is 1 atm (n=2). At room temperature, of course, the Nernst reversible potential

shifts by 4.5 mV for pH_2 = 0.75 atm. The polarization curves for p_{H2} = 1.0 atm as a function of temperature on these electrodes are shown in Figure 9. An Arrhenius analysis of these curves is shown in Figure 10 using the current densities at 20 mV versus the standard hydrogen potential in the same electrolyte.

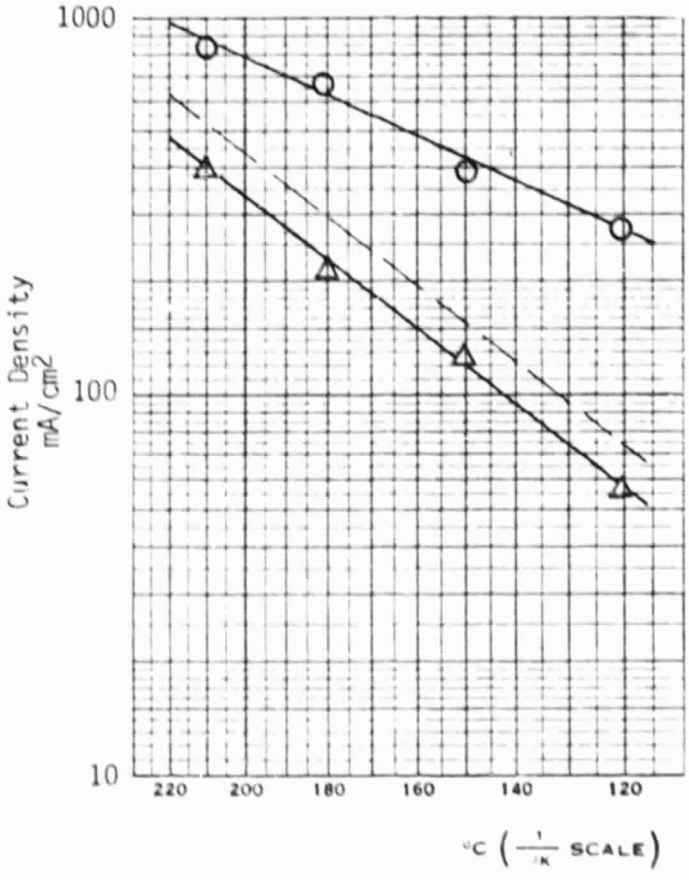

Figure 10. Arrhenius plot of hydrogen molecule oxidation at 20 mV (○). 75% H_2, 0.5% CO, 24.5% CO_2 (△). Dashed line correcting for H_2 partial pressure to give values at 100% H_2. Electrode contains 0.2 mg PGM/cm^2; 4 w/o PGM on Consel I; 50 a/o Pt, 50 a/o Pd.

Figure 10 shows the effect of temperature on the reaction rate for 75% hydrogen with 0.5% CO. These values are then corrected for the hydrogen partial pressure to show the performance values that would be obtained at 100% hydrogen. The apparent reaction rate values for hydrogen from Figure 10 are also shown at 20 mV in the absence of carbon monoxide. It can be seen that the slopes of the two sets of data (with carbon monoxide and without carbon monoxide) are different with convergence at higher temperatures. From these values it is possible to derive an apparent surface coverage of the metal electrocatalyst by the carbon monoxide poison, by comparison of the reaction rates at constant potential, and constant temperature, in the presence and absence of the carbon monoxide poison.

The purpose for deriving an apparent surface coverage of the metal electrocatalyst by a poison is to provide a determination for changes in catalyst preparation techniques, supports, and electrocatalyst materials influencing the performance criteria. In actual fact, the technically important feature for an anode electrocatalyst is the free surface on the metal particle available for reaction of the hydrogen molecule,$(1-\theta)$, rather than the poison coverage, (θ),by the carbon monoxide. The change in available electrocatalyst surface with temperature should have the function similar to the Arrhenius function, due to the similarity of the change in the equilibrium coverage, which is itself dependent upon the change in the kinetics of adsorption and desorption with temperature. The function is plotted in Figure 11. In order to compare the results on the platinum-palladium alloy electrocatalyst with platinum, we have chosen to compare the available electrocatalyst surfaces with 1% carbon monoxide in the gas stream. The original polarization curves for the methanol reformate of 75% H_2, 0.5% CO, 24.5% CO_2 as a function of temperature are shown in Figure 12 and the polarization curves for 75% H_2, 1% CO, 24% CO_2 are shown in Figure 13.

Previously, we had shown the effect of carbon monoxide poisoning for platinum supported on the turbostratic Vulcan XC-72R (Monthly Report #5, May 1980, Figure 4). Analyzing that data in a similar manner to the analysis presented here for the platinum-palladium alloys on Consel provides the change in available surface area on the platinum electrocatalysts with temperature, also shown in Figure 11.

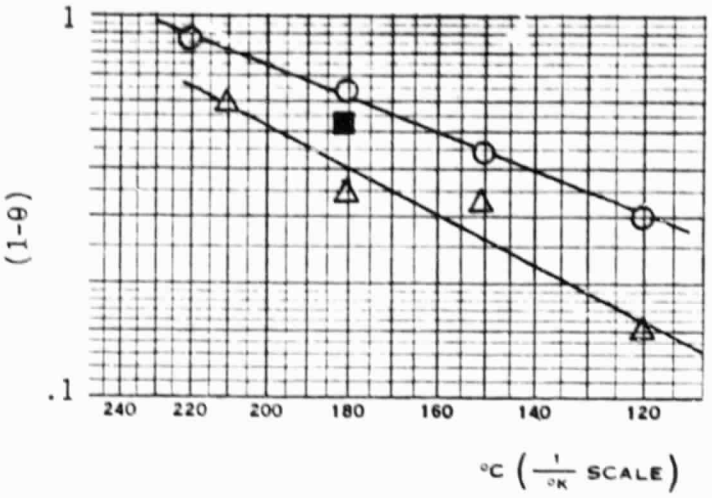

Figure 11. Available surface area on metal electrocatalysts as a function of temperature. (○), 0.5 mg Pt/cm^2 electrode, 10 w/o Pt on Vulcan XC-72R, 25 mV (DEN-3-176, May 31, 1980). (△), 0.2 mg PGM/cm^2 electrode, 4 w/o PGM on Consel I, 50 a/o Pt, 50 a/o Pd, 20 mV polarization. (■), 0.5 mg Pt/cm^2 electrode, 10 w/o Pt on Consel I. All data obtained for hydrogen oxidation in the presence of 1% CO electrocatalyst poison.

At this point, the data appear to show that in the presence of the same partial pressure of carbon monoxide, the available surface for hydrogen oxidation on platinum is greater than the available surface for hydrogen oxidation on the platinum-palladium alloy at the same temperature. In fact, such a conclusion is too simplistic since the carbon supports are quite different and the electrode structures are probably controlled by the interaction on the carbon support with the PTFE. It is also probable that the differences in the apparent available surface for the electrocatalyst are reflections of the electrolyte film within the electrode structure. Previously (Monthly Report #7, July 1980), we had carried out perturbation experiments for platinum supported on the Consel I. Variations in the Teflon content between 2.5 and 30% showed significant variations in the anode performance levels for this electrocatalyst with hydrogen oxidation in the presence of carbon monoxide. The performance curves correlated with the response of the electrode potential to perturbations. From the performance curves contained in the referenced report, the following Table is now derived.

TABLE IV

PTFE w/o	10% H_2 mA at 100 mV	10% H_2 + 1% CO mA at 100 mV	1-θ
2.5	600	60	0.1
10.0	700	52	0.07
20.0	1300	700	0.54
30.0	640	350	0.54

Table IV shows that the apparent surface coverage of carbon monoxide on platinum operating at 180°C with 10% H_2 and 1% CO, depends dramatically on the degree of wet-proofing of the electrocatalyst. Where the electrocatalyst has a thick electrolyte film at low PTFE levels, the available electrocatalyst surface for hydrogen oxidation is small. On the other hand, at high PTFE levels, the available electrocatalyst surface for hydrogen oxidation is high. The reason for this is almost certainly that with a thick electrolyte film, where the electrocatalyst is consuming the hydrogen diffusing to the surface, the localized carbon monoxide level within the electrolyte film adjacent to the metal electrocatalyst particle becomes significantly higher than the carbon monoxide level in the incoming gas stream. The performance of the electrocatalyst then becomes controlled by the ability of the carbon monoxide level within the electrolyte film to relax by diffusion from the electrocatalyst surface to the gas phase. If the electrolyte film is thick, the liquid phase diffusion restricts the ability of the electrocatalyst surface concentration to diminish; hence, the apparent poisoning becomes greater.

The value for the apparent poison coverage at high PTFE levels in Table IV is inserted into Figure 11 and shows good agreement with the sets of data. Again, it should be pointed out that this electrocatalyst contained 10 w/o Pt on the Consel support so that it has the commonality with the metal electrocatalyst for the platinum on Vulcan XC-72R values, but commonality of the support for the platinum-palladium on the Consel I support values. It has

long been recognized that electrodes made with turbostratic Vulcan XC-72R produce good electrode structures, probably due to the ability of the carbon to develop thin electrolyte films within the electrode structure when bonded with Teflon. It is concluded from the data that we have presented so far, that the poisoning characteristics and the performances of the electrodes are tremendously influenced by the electrode structure and that this goes hand in hand with the fundamental electrocatalytic activity for the metal electrocatalyst particles. The same conclusion holds for cathodes, since the feature that is important is the mass transport of the reactant molecules to the electrocatalyst surface. At the same molecular reaction rate, the mass transport from the gas phase to the electrocatalyst site will require the same concentration gradient through the electrolyte film, irrespective of the reacting species.

3.10. Task 10 - Survey of Aging

A 70-page report containing 47 figures and 124 references was completed and issued as a separate document (DOE/NASA/0176-81/3, CR 165505); consequently, no reporting on this task is in this quarterly report. Readers are invited to consult the co-issuing report.

4. Changes

There are no changes in the program.

5. Problem Areas

There are no problem areas at this time.

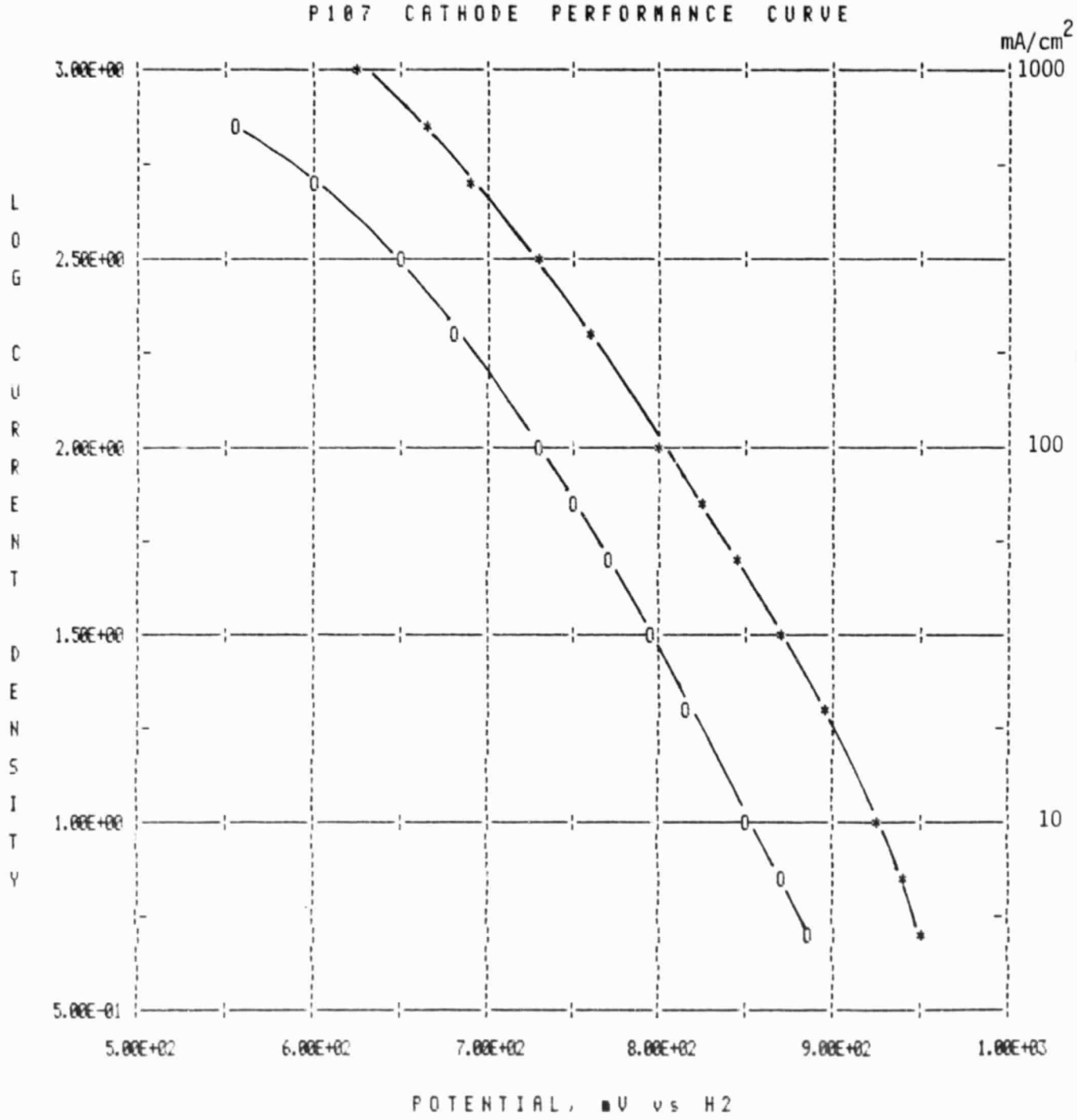

Figure 3.

Cathodic performance of electrode P-107 made from a 10%Pt/Consel IV electrocatalyst. The electrode contains 0.5mg Pt/cm^2 and was run in 100%H_3PO_4 at 100^{0}C on air(0) and O_2(*).

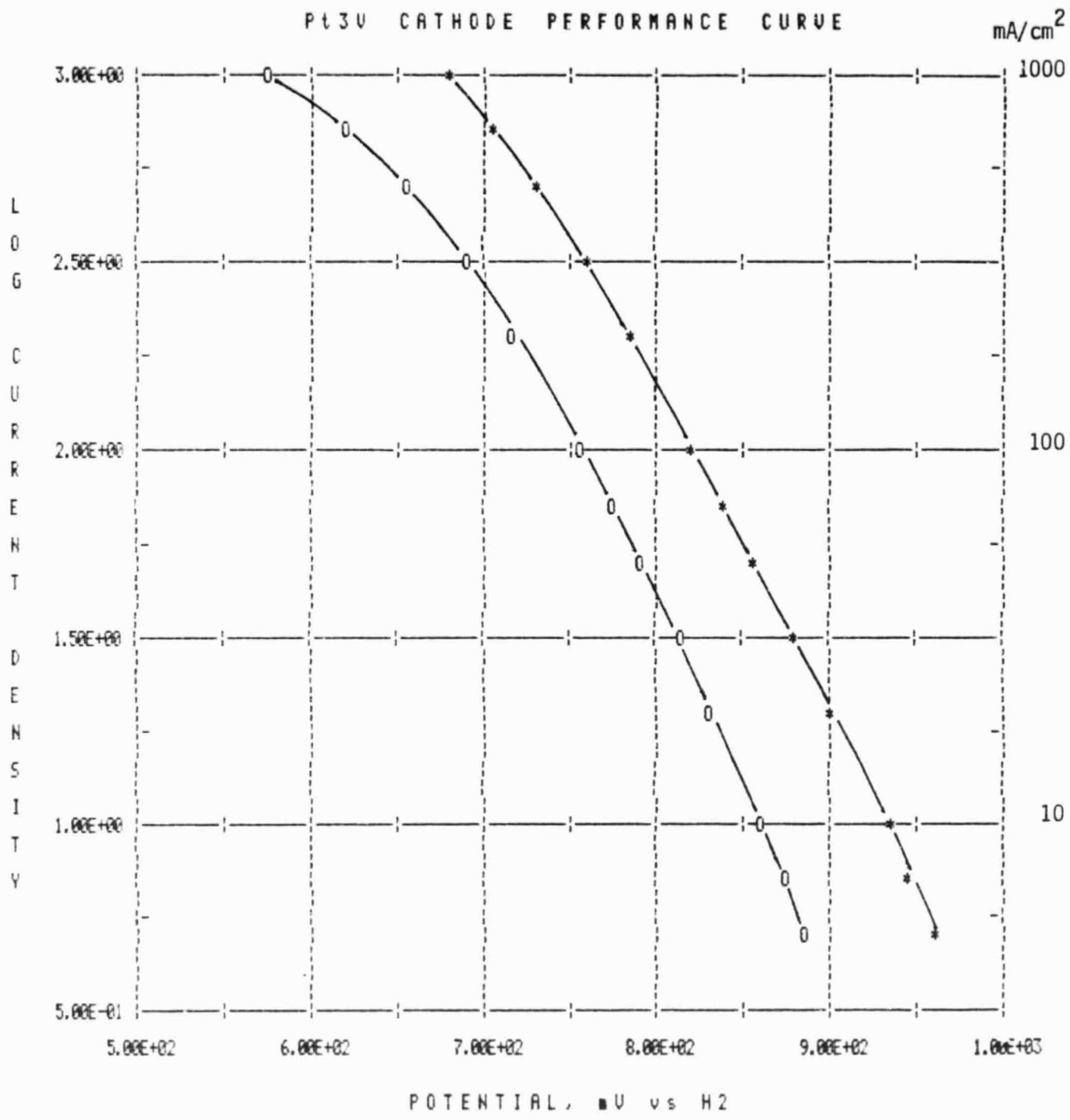

Figure 4.

Cathodic performance of electrode P-84 made from a 10.8%Pt-V/VulcanXC-72R (Pt:V ratio=11:1) electrocatalyst. The electrode contains 0.5mg Pt-V/cm^2 and was run in 100%H_3PO_4 at 180^{0}C on air(0) and O_2(*).

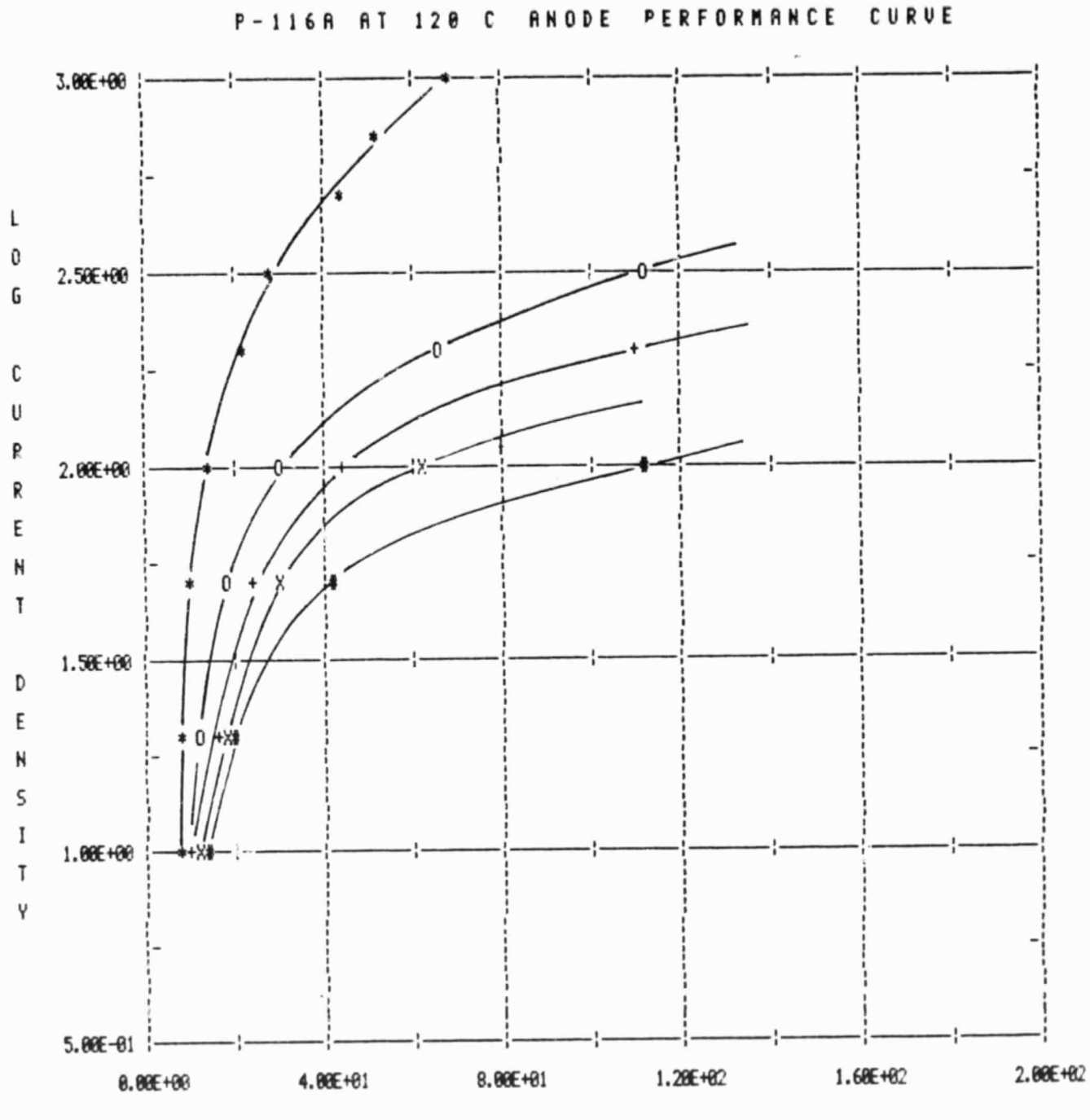

Figure 5.

Electrode Catalyst EC 123. Pt-Pd alloy (50 a/o Pt) 4 w/o PGM on Consel I. 0.2 mg PGM/cm^2 electrode, 30 w/o PTFE. (+) 75% H_2, 1% CO; (X) 75% H_2, 2% CO; (#) 75% H_2, 5% CO; (*) 75% H_2; (O) 75% H_2, 0.5% CO. Bal. N_2.

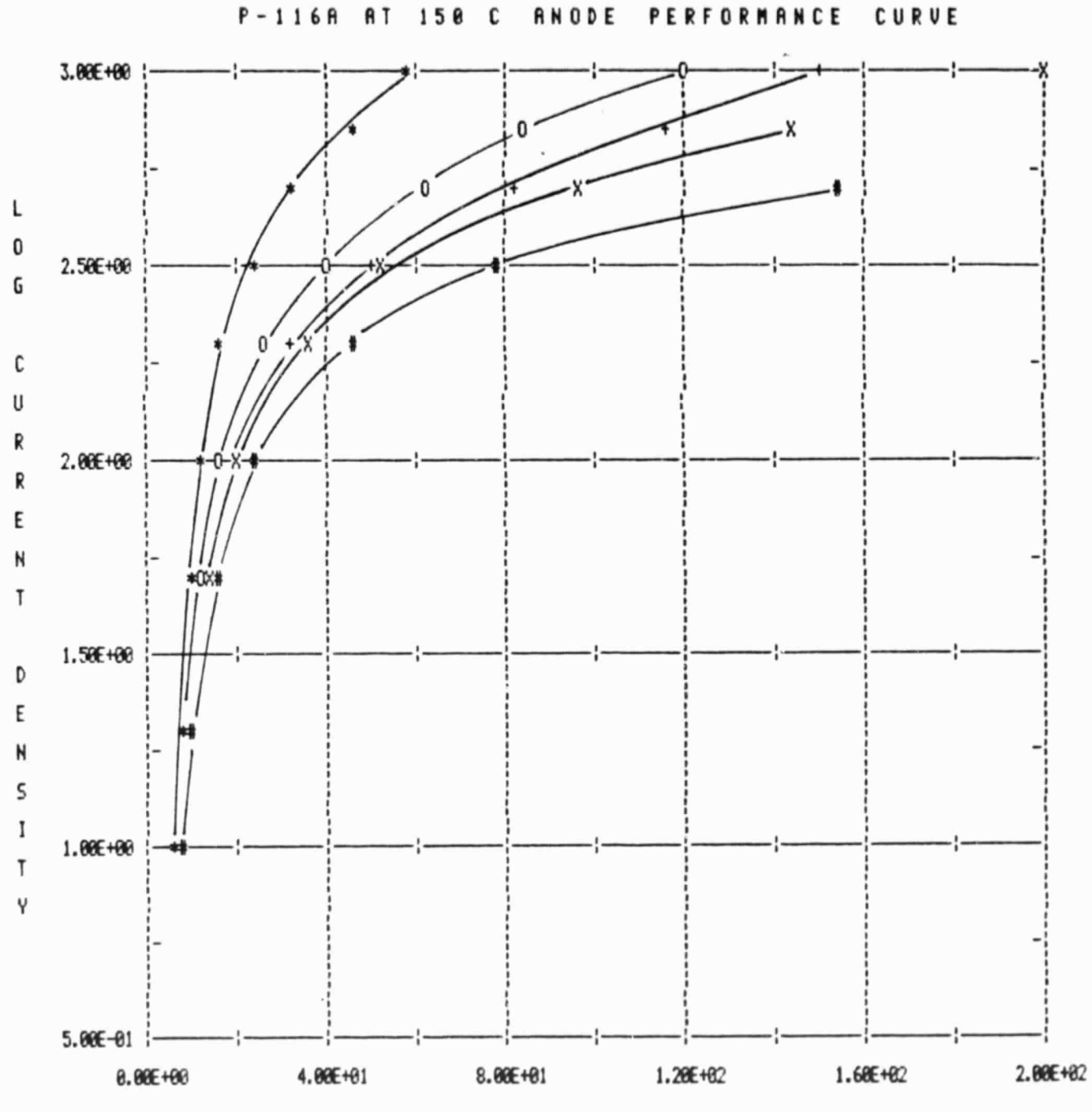

Figure 6.

Electrode Catalyst EC 123. Pt-Pd alloy (50 a/o Pt) 4 w/o PGM on Consel I. 0.2 mg PGM/cm^2 electrode, 30 w/o PTFE. (*) 75% H_2; (0) 75% H_2, 0.5% CO; (+) 75% H_2, 1% CO; (X) 75% H_2, 2% CO; (#) 75% H_2, 5% CO. Bal. N_2.

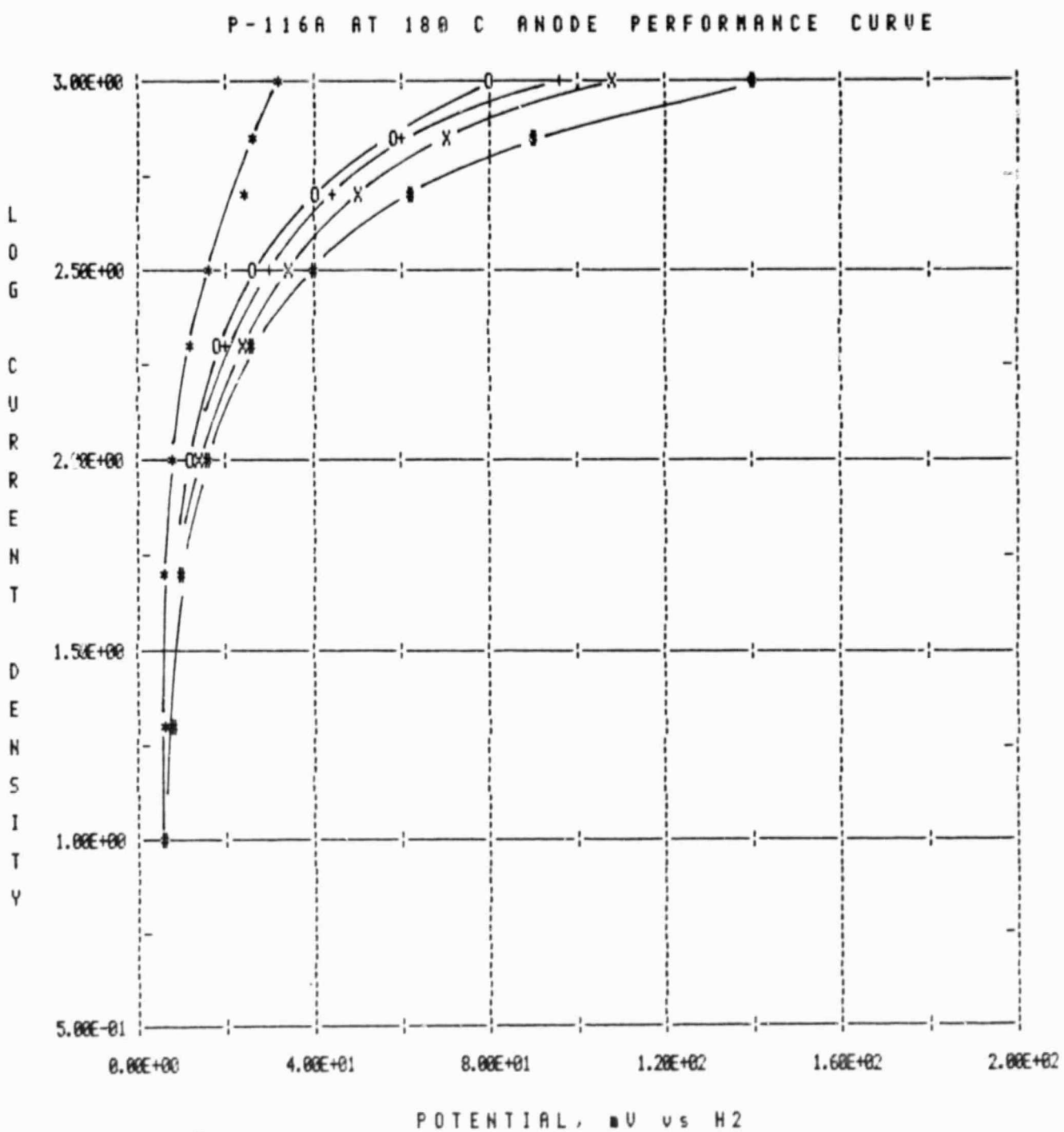

Figure 7.

Electrode Catalyst EC 123. Pt-Pd alloy (50 a/o Pt) 4 w/o PGM on Consel I. 0.2 mg PGM/cm^2 electrode, 30 w/o PTFE. (*) 75% H_2; (0) 75% H_2, 0.5% CO; (+) 75% H_2, 1% CO; (X) 75% H_2, 2% CO; (#) 75% H_2, 5% CO. Bal. N_2.

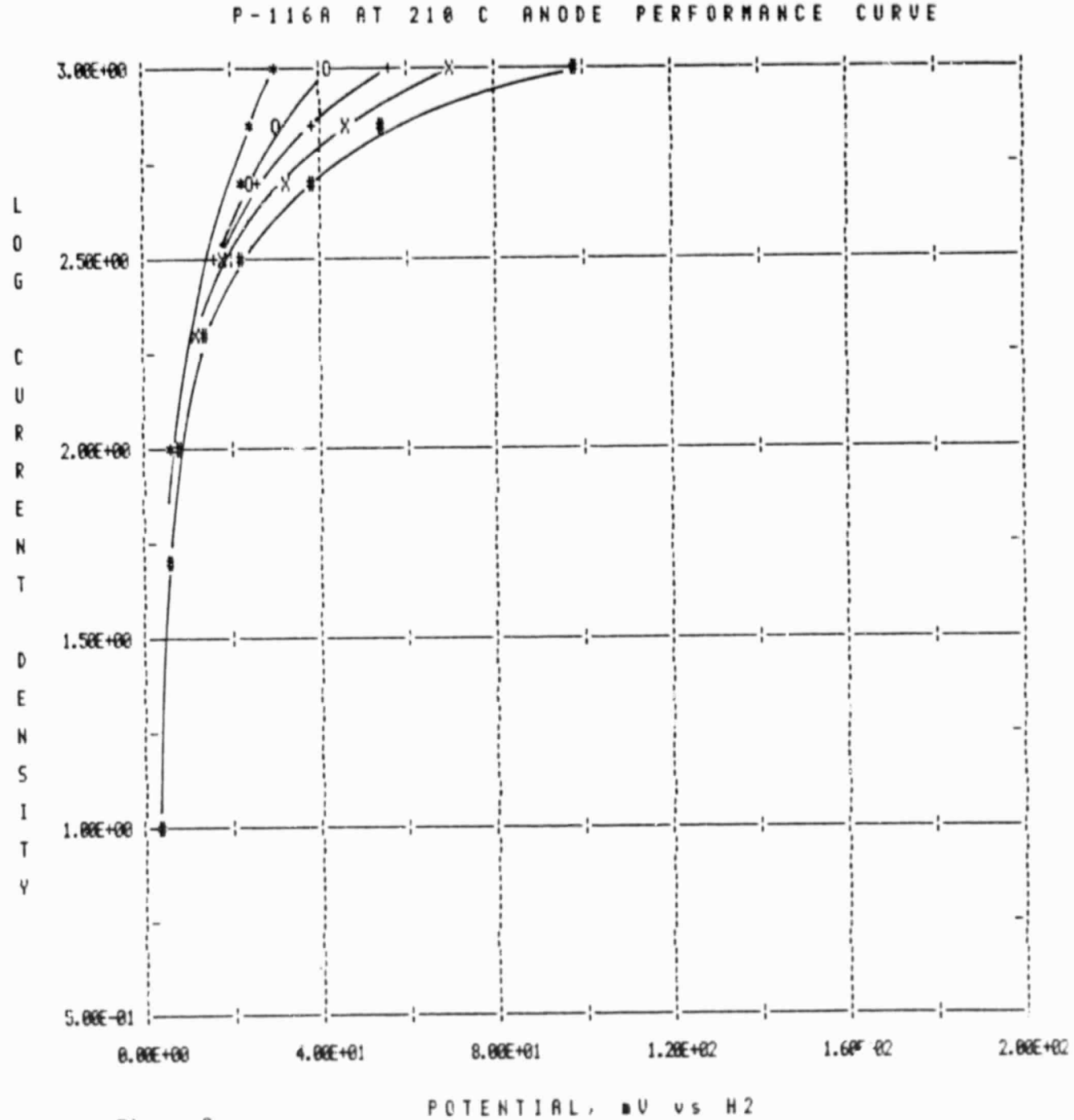

Figure 8.

Electrode Catalyst EC 123. Pt-Pd alloy (50 a/o Pt) 4 w/o PGM on Consel I. 0.2 mg PGM/cm^2 electrode, 30 w/o PTFE. (*) 75% H_2; (O) 75% H_2, 0.5% CO; (+) 75% H_2, 1% CO; (X) 75% H_2, 2% CO; (#) 75% H_2, 5% CO. Bal. N_2.

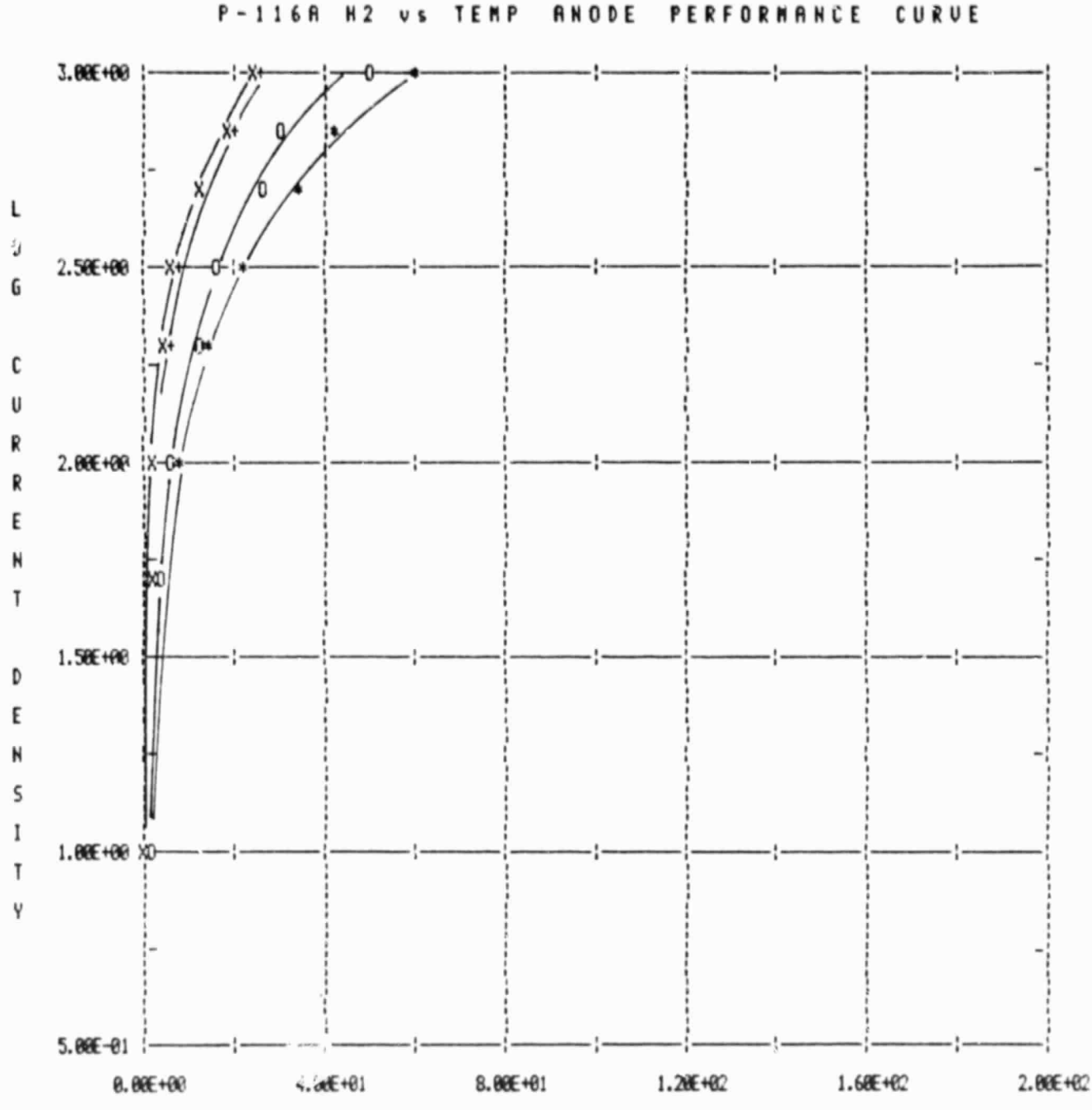

Figure 9.

Electrode Catalyst EC 123. Pt-Pd alloy (50 a/o Pt) 4 w/o PGM on Consel I. 0.2 mg PGM/cm^2 electrode, 30 w/o PTFE. 1 atm. H_2.
(X) 210°C; (+) 180°C; (0) 150°C; (*) 120°C.

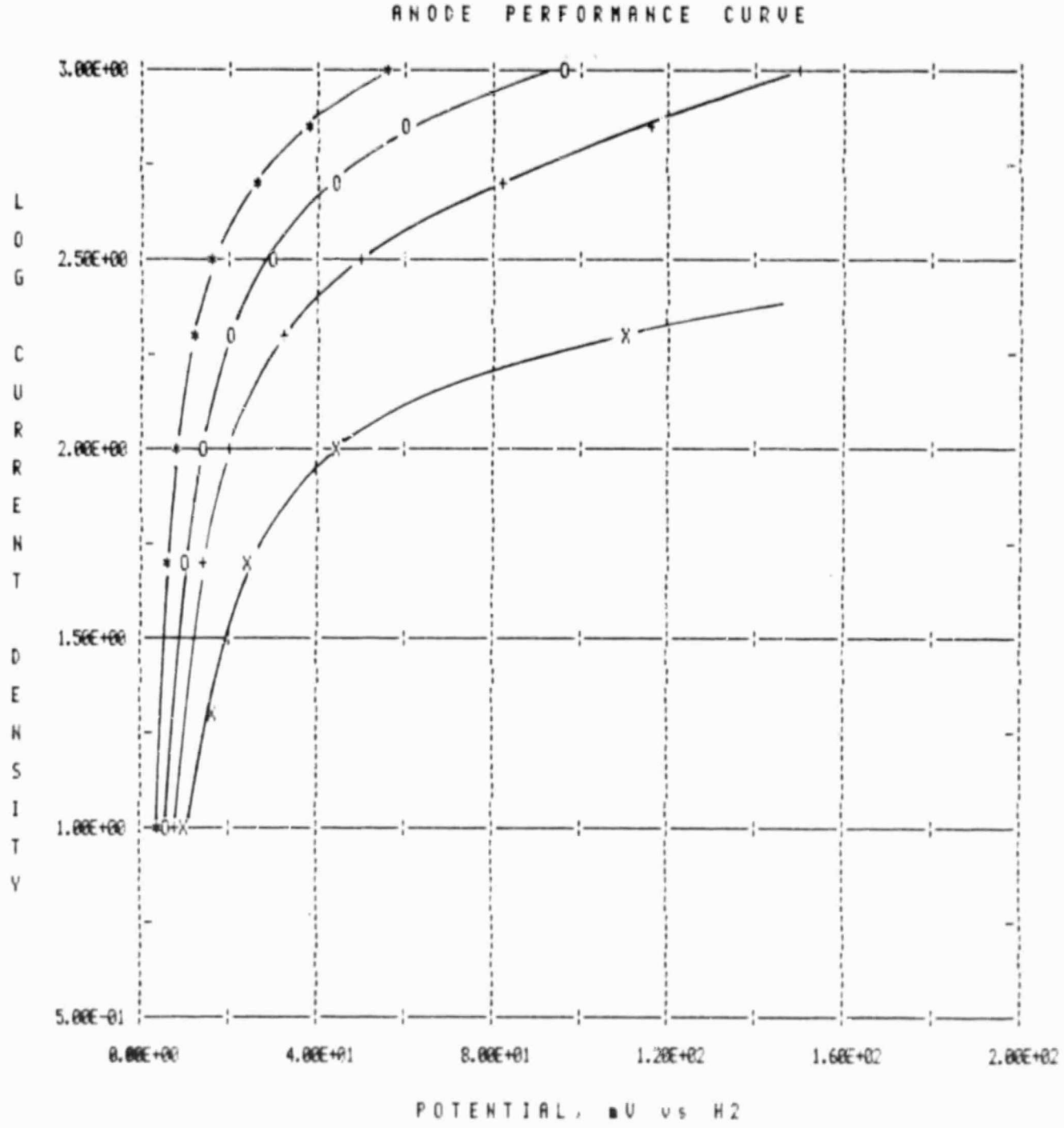

Figure 12.

Electrode Catalyst EC 123. Pt-Pd alloy (50 a/o Pt) 4 w/o PGM on Consel I. 0.2 mg PGM/cm^2 electrode, 30 w/o PTFE. Performance characteristics for 75% H_2,24% N_2, 1% CO. (X) 210°C; (+) 180°C; (0) 150°C; (*) 120°C.

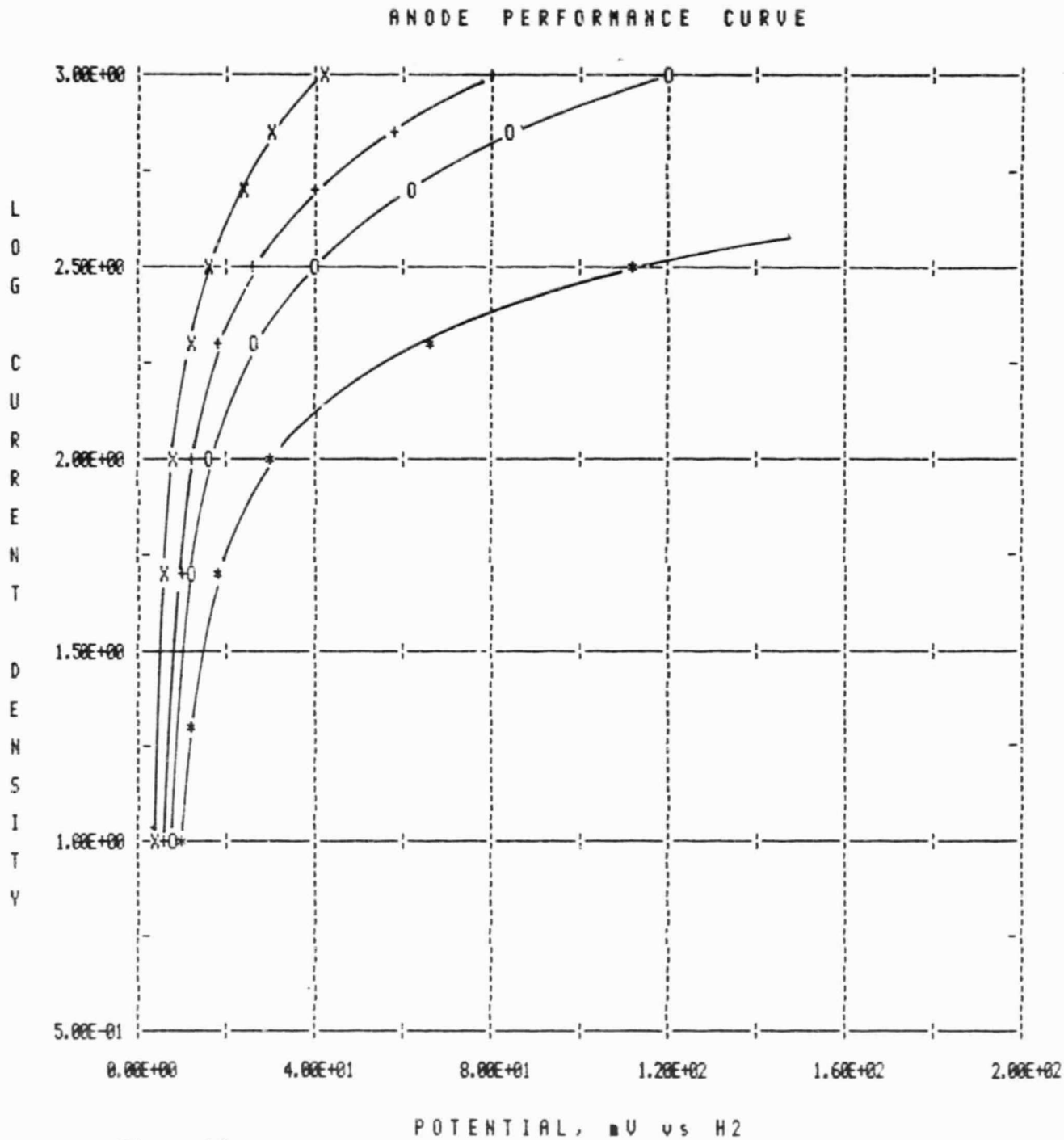

Figure 13.

Electrode Catalyst EC 123. Pt-Pd alloy (50 a/o Pt) 4 w/o PGM on Consel I. 0.2 mg PGM/cm^2 electrode, 30 w/o PTFE. Performance characteristics for 75% H_2, 24½% N_2, 0.5% CO. (X) 210°C; (+) 180°C; (O) 150°C; (*) 120°C.

APPENDIX - DERIVATION OF EQUATION 1

Crystallite size determination by voltammetry requires measuring the pseudocapacity associated with the adsorption of hydrogen on the surface of the crystallites. For palladium crystallites there is not only a pseudocapacity associated with hydrogen adsorption on the crystallite surface, but also a pseudocapacity due to the absorption of hydrogen into the interior of a palladium crystallite. The ratio of hydrogen to palladium atoms on the surface can reasonably be assumed to be 1:1. For absorbed hydrogen, the hydrogen to palladium ratio has been reported to be less than 1:1 and depends upon temperature and hydrogen partial pressure (Palcyewska, Advances in Catalysis, 24, 248, 1975).

Using spherical geometry, a relationship between crystallite size and hydrogen adsorption plus absorption pseudocapacitance can be developed using an arbitrary value for R, the ratio of hydrogen to palladium for absorbed hydrogen. The value of R can be determined by correcting potentiodynamic hydrogen pseudocapacity to microscopically determined cyrstallite size.

The total pseudocapacitive charge (Q) on one gram of palladium crystallite is:

$$Q = \#cQ_c \tag{1}$$

where Q_c is the charge per crystallite and #c is the number of crystallites per gram.

$$\#c = V_T/V_c \tag{2}$$

where V_T is the total volume of one gram of palladium and V_c is the volume of an average crystallite.

If I_a equals the number of internal atoms in a crystallite and S_a equals the number of surface atoms in a crystallite:

$$Q_c = I_aRe + S_ae \tag{3}$$

where e is the charge per hydrogen atom ($e = 1.602 \times 10^{-19}$ coul.) and R is the H/Pd ratio for internal Pd atoms.

$$I_a = T_a - S_a \tag{4}$$

(T_a = total atoms in a crystallite)

Therefore:

$$Q_c = (T_a - S_a)\, Re + S_a e \tag{5}$$

or:

$$Q_c = \{T_a R + S_a\,(1-R)\}e \tag{6}$$

The value of T_a can be determined from V_c, the volume of a crystallite, and V_a, the volume of a single atom.

$$T_a = V_c / V_a \tag{7}$$

The value of S_a is determined by:

$$S_a = A_c / A_{ac/s} \tag{8}$$

where A_c is the surface area of a crystallite and $A_{ac/s}$ is the cross sectional area of a single atom.

Therefore:

$$Q_c = \left(\frac{V_c}{V_a} R + \frac{A_c}{A_{a\ c/s}} \,(1 - R) \right) e \tag{9}$$

and since $Q = \#cQ_c$:

$$Q = \frac{V_T}{V_c} \left(\frac{V_c}{V_a} R + \frac{A_c}{A_{a\ c/s}} (1 - R) \right) e \tag{10}$$

or:

$$Q = \left\{ \frac{V_T}{V_a} R + \frac{V_T}{V_c} \cdot \frac{A_c}{A_{c\ c/s}} (1 - R) \right\} e \qquad (11)$$

Using the following relationships: (d_c = crystallite diameter; d_a = atom diameter):

$$V_T = 1/p \qquad A_c = \pi d_c^2 \qquad A_{a\ c/s} = \frac{\pi d_a^2}{4}$$

$$V_a = M/Np \qquad V_c = \frac{\pi d_c^3}{6}$$

where M = molecular weight; N = Avagadro's number; p = density.

Equation (11) becomes:

$$Q = \frac{NRe}{M} + \frac{(1-R)e}{d_c} \left(\frac{24}{\pi p}\right) \left(\frac{\pi NP}{6M}\right)^{2/3} \qquad (12)$$

or setting:

$$A = \frac{Ne}{M} \text{ and } B = \left(\frac{24}{\pi p}\right) \left(\frac{\pi NP}{6M}\right)^{2/3} e \qquad (13)$$

$$Q = AR + \frac{(1-R)}{d_c} B \qquad (14)$$

or

$$d_c = \frac{B(1-R)}{Q-AR} \qquad (15)$$

To obtain d_c in $\mathring{A}$ use:

$$A = 9.07 \times 10^2 \text{ and } B = 1.10 \times 10^4$$